

## Yield stress of monocrystalline rhenium nanowires

L. Philippe,<sup>a)</sup> I. Peyrot, and J. Michler  
EMPA (Laboratories for Materials Technology), Feuerwerkerstrasse 39, CH-3602 Thun, Switzerland

A. W. Hassel and S. Milenkovic  
Max-Planck Institute für Eisenforschung, Max-Planck-Strasse 1, D-40237 Düsseldorf, Germany

(Received 19 June 2007; accepted 27 August 2007; published online 14 September 2007)

The yield stress of monocrystalline Rhenium nanowires grown by directional solidification was measured by nanobending testing. The average yield stress calculated from the deflection was between 10 and 60 GPa, which represents roughly 10% of the rhenium Young modulus along the nanowire's direction. Analytical results are compared to the ones obtained with a more complex finite element simulation. Origins of the experimental observed yield stress values variations are discussed in terms of experimental measurement errors, elastic anisotropy, and the presence of an oxide layer on the nanowire surface. © 2007 American Institute of Physics.

[DOI: 10.1063/1.2785153]

Metal nanowires (NWs) have stimulated great interest because of their high thermal and electrical conductivities and high strength.<sup>1-3</sup> In recent years, a collection of experimental yield stress measurement has been collected but limited mainly to noble and monocrystalline NWs. However, nothing is known about the mechanical properties of other non-noble metallic materials, including rhenium, and this has limited their applications in constructing reliable nanodevices. It is clearly suspected that in the engineering of metallic NW, the nanostructure and its surface state (native oxide state) plays a significant role in the strength of the nanowires.<sup>4,5</sup> Finally, only face-centered cubic nanostructures have been investigated so far. Mechanical properties of hexagonal structures such as for rhenium, where only few glide planes are active compared to Ag or Au and where dislocations behavior are different from FCC systems,<sup>6</sup> need to be studied.

In this paper, we present bending experiments on monocrystalline rhenium (Re) nanowires that were produced by directional solidification of an eutectic NiAl-Re alloy and subsequent selective etching of the NiAl matrix.<sup>7</sup> By direct observations and using elasticity theory as well as the finite element method, the yield stress of the Re NW is determined. We show that the yield stress of the material is up to 100 times higher than that for the bulk counterpart. An estimation of the experimental error is made and a numerical study of the intrinsic effect of the material anisotropy and native oxide layer effect on the measured properties is given.

For the measurements, an atomic force microscopy (AFM) cantilever was set up inside the chamber of a scanning electron microscope (see Ref. 2 for more details). The AFM tip was used for bending individual rhenium NWs that were standing perpendicularly to the substrate. The whole procedure, which was captured to a video file, described the different deformation stages of the rhenium NW: elastic, elastoplastic, and fracture. The maximal displacement  $s$  corresponding to the NW deformation just before the plastic limit was then measured through image analysis. On each measured dimension, the image tilt was corrected.

We suppose that a monocrystalline NW with one locally perpendicular fixed extremity to the substrate deforms elastically at a point  $x$  before plastic deformation. This allows us to use the elastic, isotropic beam theory. The maximal tensile  $(\sigma_z)_{\max}$  occurs when the NW is clamped at  $z=0$ ,  $x=-w/2$  ( $w$  being the width of NW) and can be written as

$$(\sigma_z)_{\max} = \frac{3w}{2L^2}Es, \quad (1)$$

where  $s$  is the deflection of the NW,  $L$  is the total NW length, and  $E$  is the elastic modulus of the material. Error sources that are intrinsic to dimension measurements used for solving Eq. (1) are estimated to be of a maximum error of 15% for the width  $w$ , the length  $L$  of the NW, and the measured displacement  $s$  (see Ref. 2 for details). The relative experimental error  $(\Delta\sigma/\sigma)$  in the yield stress can be written as

$$\frac{\Delta\sigma_{\max}}{\sigma_{\max}} = \left| \frac{\Delta w}{w} \right| + 2 \times \left| \frac{\Delta L}{L} \right| + \left| \frac{\Delta s}{s} \right|. \quad (2)$$

The estimated error in the measurement of the yield stress is therefore approximately  $\pm 60\%$ . Table I shows very significant differences in yield stress for the different wire dimensions that were measured, largely beyond the estimated measurement errors. It is not possible to conclude if this size effect should be linked to the length, the surface, or the volume of the tested nanostructures taking into account the possible anisotropy of the wires or eventual defects. The calculated analytical yield stress is substantially higher (up to 100

TABLE I. Measured yield stress  $(\sigma_z)_{\max}^{ana}$  of the Re NWs calculated by means of the simple beam formula [Eq. (1)]. The Young modulus of the Re NW is fixed at 472.59 GPa.

| NW | $L$ ( $\mu\text{m}$ ) | $w$ ( $\mu\text{m}$ ) | $w/L^2$ ( $\mu\text{m}$ ) | $s$ ( $\mu\text{m}$ ) | $(\sigma_z)_{\max}^{ana}$ (GPa) |
|----|-----------------------|-----------------------|---------------------------|-----------------------|---------------------------------|
| 1  | 6.8                   | 0.7                   | $1.5 \times 10^{-2}$      | 5.6                   | $65 \pm 39$                     |
| 2  | 7.8                   | 0.5                   | $8.2 \times 10^{-3}$      | 7.8                   | $48 \pm 29$                     |
| 3  | 11.2                  | 0.5                   | $3.9 \times 10^{-3}$      | 8.2                   | $25 \pm 15$                     |
| 4  | 11.8                  | 0.5                   | $3.5 \times 10^{-3}$      | 4.9                   | $12 \pm 7.2$                    |
| 5  | 14.3                  | 0.5                   | $2.4 \times 10^{-3}$      | 7.8                   | $15 \pm 9$                      |
| 6  | 15.2                  | 0.5                   | $2.2 \times 10^{-3}$      | 6.4                   | $10 \pm 5.8$                    |
| 7  | 12.2                  | 0.3                   | $2.0 \times 10^{-3}$      | 5.2                   | $8 \pm 4.7$                     |

<sup>a)</sup> Author to whom correspondence should be addressed; electronic mail: laetitia.philippe@empa.ch

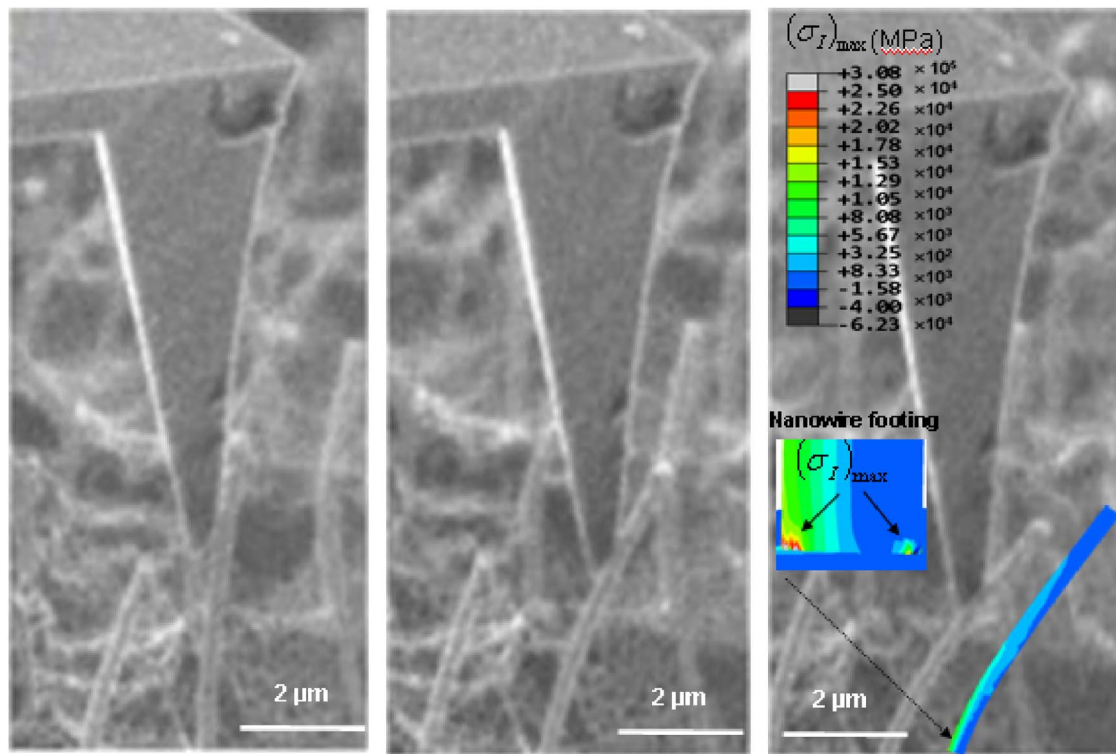


FIG. 1. (Color online) FE Simulation of NW bending. Bending experimental image sequences from elastic to plastic NW deformation overlaid with FE simulation picture for NW dimension. The maximal principal stress  $(\sigma_I)_{\max}$  occurs when the NW is thicker (nanowire footing).

times higher) than the value of the bulk rhenium (255–317 MPa at room temperature reported in literature). For all NWs tested, we calculate a value that varies between  $E/7$  and  $E/60$ , where  $E/10$  corresponds to the theoretical value of fracture strength for rhenium.

Three dimensional anisotropic FE simulations using the commercial FE program ABAQUS®/STANDARD (standard version 6.4, HKS, Inc., Pawtucket, RI) were performed to check the validity of the simple beam formula with respect to large deflections, anisotropy, and oxide layer. The hexagonal shape of the NW is used for discretization. A bilateral sticking contact between the tip and the NW is assumed. We consider rhenium with a purely elastic behavior. The Poisson's ratio  $\nu$  is always fixed at 0.3. For this anisotropic material, the stiffness tensor  $C$  is described with five independent elastic constants  $c$  (equal to  $c_{11}=618.2$  GPa,  $c_{12}=275.3$  GPa,  $c_{13}=207.8$  GPa,  $c_{33}=683.5$  GPa, and  $c_{44}=160.6$  GPa).<sup>8,9</sup> The material grows in the  $\langle 2023 \rangle$  direction. With a rotation of the matrix  $C$ , we evaluate the Young modulus of rhenium to 472.59 GPa in this direction. Figure 1 overlays a picture of a bended NW (in the elastic region) with the FE simulation for the same structure: both exhibit a similar deformation profile. Note that a high stress concentration at the NW footing related to the increased moment of area of the NW is simulated. Figure 2 shows that numerical and analytical yield stress values are in good agreement with each other, which indicates the validity of using the elastic beam theory for the evaluation of the yield stress of the NWs. It seems that the Re NW cross-sectional geometry does not influence significantly the yield stress values obtained. In the following, the study will use NW geometric characteristics described by the simulation (c).

NiAl substrate is now taken into account in the FE simulation. The substrate is modeled as an elastic material ( $E$

=188 GPa and  $\nu=0.3$ ).<sup>10</sup> Table II gives a comparison between the numerical yield stress measured by considering a clamped beam  $[(\sigma_z)_{\max}^n]$  and the one which takes into account the substrate  $[(\sigma_z)_{\max}^{n+s}]$ . The relative error in yield stress varies between 2.5% and 24%, which underlines that the nature of the substrate influences to a certain extent the evaluation of the yield stress.

The Re NWs anisotropic behavior is studied now by considering the system as an attached beam and neglecting the substrate effect. For ABAQUS®/STANDARD, this type of behavior makes the elastic stiffness matrix  $C$  associated with

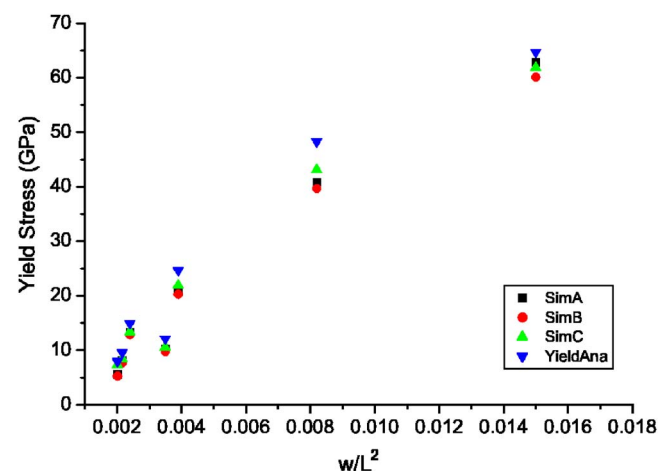


FIG. 2. (Color online) Comparison of yield stress  $(\sigma_z)_{\max}^{ana}$  of the Re NWs calculated with the simple beam formula [Eq. (1)] and by the FEMs  $(\sigma_z)_{\max}^{n(A,B,C)}$  FE taking into account the different geometrical NWs configuration, as a function of  $w/L^2$ : (A) considers a cubic cross-section ( $t=w$ ) of the wire (B) considers a rectangular cross section ( $t=w/2$ ), and (C) considers a cubic cross section with rounded angles.

TABLE II. Comparison of measured yield stress ( $\sigma_z^n$ ) of the Re NWs calculated by the FEMs taking into substrate properties ( $\sigma_z^{n+s}$ ) and anisotropic properties of the system ( $\sigma_z^{n+a}$ ).

| NW | $L$ ( $\mu\text{m}$ ) | $w$ ( $\mu\text{m}$ ) | $(\sigma_z^n)_{\text{max}}$ (GPa) | $(\sigma_z^{n+s})_{\text{max}}$ (GPa) | $(\sigma_z^{n+a})_{\text{max}}$ (GPa) |
|----|-----------------------|-----------------------|-----------------------------------|---------------------------------------|---------------------------------------|
| 1  | 6.8                   | 0.7                   | 62                                | 66                                    | 60                                    |
| 2  | 7.8                   | 0.5                   | 43                                | 48                                    | 41                                    |
| 3  | 11.2                  | 0.5                   | 22                                | 30                                    | 20                                    |
| 4  | 11.8                  | 0.5                   | 11                                | 12                                    | 10                                    |
| 5  | 14.3                  | 0.5                   | 14                                | 15                                    | 13                                    |
| 6  | 15.2                  | 0.5                   | 8                                 | 9                                     | 8                                     |
| 7  | 12.2                  | 0.3                   | 7                                 | 7                                     | 6                                     |

the initial material's principal orientation  $\langle 20\bar{2}3 \rangle$ . Table II compares the measurement of the yield stress in the case of an isotropic  $(\sigma_z^n)_{\text{max}}$  and an anisotropic  $(\sigma_z^{n+a})_{\text{max}}$  Re NW. Clearly, the anisotropic properties of the structure plays a significant role on its resulting yield stress value with a relative error up to 15% in certain cases. More interestingly, anisotropy effects on the measured yield stress and depending on the load orientation applied to the NW are shown on Fig. 3. Here, both substrate and anisotropic influence are implemented using the dimensions of NW1 (see Table I). The angle of the load applied by the AFM tip on the NW results in the variation of the measured yield stress fluctuating by more than 65%.

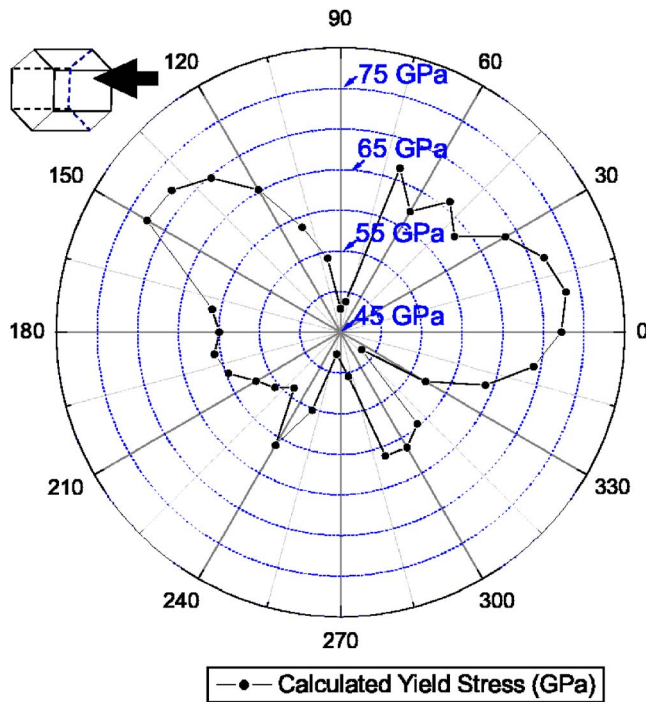


FIG. 3. (Color online) Measured yield stress ( $\sigma_z^{n+a}$ ) calculated by FEM as a function of the loading direction for NW1. The inset shows the hexagonal structure orientation.

The etching procedure applied to reveal freestanding Re NW out of the NiAl has an effect on the Re NW surface and most probably favors growth of an oxide layer ( $\text{ReO}_2$ ) and ( $\text{ReO}_3$ ) on the material. The mechanical properties of the rhenium oxide layer have not been investigated and no data exist about its mechanical behavior. We assumed a sticking contact between the oxide and rhenium, an oxide layer thickness equal to 4 nm equally distributed around the NW, the same dimensions of the system (oxide+rhenium) as NW2 (see Table I), and an arbitrary elastic behavior with a stiffness value of the oxide of 150 GPa. In this case, we find a yield stress value of 33 GPa, compared to 48 GPa while neglecting the surface oxide state presence. This shows the importance of modeling the oxide in order to avoid an underestimation of the yield stress value.

To Summarize, the mechanical properties of Re monocrystalline NWs with a hexagonal crystal structure have been evaluated. Numerical and analytical findings report yield stress values between 10 and 60 GPa for Re NW, which represents roughly 10% of the Young modulus value and until 100 times higher than the one reported for its bulk counterpart. Discrepancies and errors intrinsic to the experimental data clearly underline the importance of an advanced numerical model to measure the yield stress of NWs with accuracy. Effects of substrate stiffness, anisotropy, and surface state properties of the system were investigated. The finite element model shows that these effects have to be taken into account for accurate determination of the mechanical properties.

Financial support by the European Commission in the frame of the project HYDROMEL is gratefully acknowledged. Special thanks go to Nanonis GmbH, Zürich, Switzerland and S. Hoffmann (EMPA) for advice related to the realization of the experimental setup. Two of the authors (L.P. and I.P.) contributed equally to this work.

- <sup>1</sup>A. San Paulo, J. Bokor, R. T. Howe, R. He, P. Yang, D. Gao, C. Carraro, and R. Maboudian, *J. Appl. Phys.* **87**, 053111 (2005).
- <sup>2</sup>S. Hoffmann, I. Utke, B. Moser, J. Michler, S. H. Christiansen, V. Schmidt, S. Senz, P. Werner, and U. Gösele, *Nano Lett.* **6**, 622 (2006).
- <sup>3</sup>S. Fahlbusch, S. Mazerolle, J.-M. Breguet, A. Steinecker, J. Agnus, R. Pérez, and J. Michler, *J. Mater. Process. Technol.* **167**, 371 (2005).
- <sup>4</sup>B. Wu, A. Heidelberg, J. J. Boland, J. E. Sader, X. Sun, and Y. Li, *Nano Lett.* **6**, 468 (2006).
- <sup>5</sup>W. Ding, L. Calabri, X. Chen, K. M. Kohlhaas, and R. S. Ruoff, *Compos. Sci. Technol.* **66**, 1112 (2006).
- <sup>6</sup>D. Hull and D. J. Bacon, *Introduction to Dislocations* (Butterworth Heinemann, Oxford, 2006), Vol. 5, pp. 83–101.
- <sup>7</sup>A. W. Hassel, B. Bello Rodriguez, S. Milenkovic, and A. Schneider, *Electrochim. Acta* **51**, 795 (2005).
- <sup>8</sup>D. R. Lide, *Handbook of Chemistry and Physics*, 86th ed. (Taylor and Francis, Boca Raton, FL., 2005), Vol. 12.
- <sup>9</sup>J. F. Nye, *Physical Properties of Crystal* (Clarendon, Oxford, 1960), Vol. 8, pp. 131–148.
- <sup>10</sup>R. J. Wasikewski, *Trans. AIME* **236**, 455 (2005).